A Fourier transform microscope for x-ray imaging

K. S. Wood, U. Feldman, and P. A. Becker
Naval Research Laboratory, Washington, D.C. 20375-5000

R. J. Nemiroff
NASA/Goddard Space Flight Center, Greenbelt, Maryland 20771

D. R. Kania
Lawrence Livermore National Laboratory, Livermore, California 94550

(Presented on 18 March 1992)

This is a progress report on development of a new x-ray imaging system, called a Fourier transform microscope, intended for use with x-ray emitting targets in laser fusion experiments. It is being built by Naval Research Laboratory and Lawrence Livermore National Laboratory. The system works at energies from 3 to 7 keV. We describe the development of the design, which utilizes fine etched grids to extract Fourier amplitudes for the source brightness distribution at selected spatial frequencies. The finest grids in the prototype system will have rib dimensions of 2 μm. The prototype system is expected to achieve position resolution of 4 μm in 3–7 keV. Simulations of the expected imaging performance are presented.

I. INTRODUCTION

We present here a new concept for x-ray imaging microscopes capable of extracting high-resolution spatial information, and describe development of a prototype version of such an instrument now being undertaken by the Naval Research Laboratory (NRL) and the Lawrence Livermore National Laboratory (LLNL). The instrument can be used as an imaging tool in support of inertial confinement fusion (ICF) experiments. For example in direct-drive ICF experiments, a target compressed to less than 100 μm in size radiates copious x rays for a short time. For diagnostic purposes it is desirable to map such targets on spatial scales of a few microns if possible. The mapping can be either two-dimensional (for imaging purposes) or one-dimensional (for direct measurement of Fourier amplitudes in Rayleigh Taylor experiments). Previous attempts to obtain images using conventional pinhole techniques yielded low throughput with insufficient resolution. We summarize below the relevant new features of the Fourier transform microscope (FTM).

A. Motivations

There are a number of techniques for x-ray microscopy at energies below 3 keV using mirrors or Fresnel zone plates. X-ray reflective optics methods work poorly at energies above a few keV because mirror reflectivity becomes small for photons at those energies, hence the length of the optical surfaces required to achieve grazing incidence reflection increases steeply with energy, and eventually becomes prohibitive. In practice mirror systems have trouble providing desired spatial resolution (below 10 μm) at energies $E > 3$ keV. Fresnel zone plates suffer from a double drawback at high energies: in the plane of the zone plate the spacing of opaque and transparent regions becomes very small (typically < 0.1 μm) but in the direction perpendicular to the plate x-ray opaque regions must be thick enough to be absorbing at the intended operating energy which means in practice they must be considerably thicker than 1 μm. The ratio of spacing to thickness becomes a source of practical difficulty. Zone plates also have a narrow operating range in energy, a drawback in some applications.

In situations where the source to be imaged is fairly large or the spatial scale to be imaged is not very fine, so that detectors exist with position resolution comparable to the desired spatial resolution in the image, it is possible to use the technique of coded aperture imaging to obtain a source image. In such cases there is a single mask with multiple apertures (or "pinholes") placed between the source and the position-sensitive x-ray detector. The detector records a transform of the source image that can be inverted by suitable image reconstruction methods. This method will not provide imaging at scales much finer than the finest scale measurable with the detector. The metrology of the alignment of the detector and the masks determines the precision to which the reconstructed image can be positioned. The limitations of the techniques described above have motivated the authors to examine the viability of adapting astronomical Fourier transform imaging techniques to extract diagnostics in laboratory fusion experiments.

B. FTM concept

A Fourier transform microscope is a new type of x-ray coded aperture microscope. Coded apertures[1,2] are extensions of the idea of a pinhole camera. X rays passing through the aperture to a detector (film or electronic) encounter a pattern of opaque and transparent regions arranged so that the detector records a transform of the source brightness distribution. Inverting this transform recovers the brightness distribution. In the case of the FTM the mathematical basis is the Fourier transform. The microscope is made of elements each of which measures a different spatial Fourier component of the brightness distribution.

 0034-6748/92/105089-05$02.00

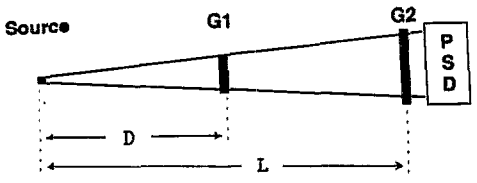

FIG. 1. Major subassemblies of FTM.

Fourier transform imaging has been used previously in radio astronomy.[3,4] We define the Fourier transform of the source brightness distribution as

$$\tilde{I}(u,v)=\int_{-\infty}^{\infty}\int_{-\infty}^{\infty} dxdyI(x,y)e^{i(ux+vy)},$$

where (u,v) is the wave number vector. Note that the transform $\tilde{I}(u,v)$ possesses both a real and an imaginary part; the amplitude and phase of the transform are then given by $\tilde{A}=|\tilde{I}(u,v)|$ and $\Phi=\arg \tilde{I}(u,v)$, respectively. In radio astronomy applications interferometers (e.g., pairs of antennae along various baselines) are used to extract Fourier components. The number of baselines is increased until there are enough measured components for satisfactory image reconstruction. For x rays, modulation collimators[5,6] and other designs utilizing arrangements of grids[7] have been employed. The principle of operation in the x-ray cases more nearly resembles the microscope described here but the inversion software to recover the image from the measured Fourier amplitudes is essentially the same in the two cases. The microscope design detailed here optimally arranges grids that themselves represent the state of the art in x-ray opaque grid fabrication into a system that provides the required fine-scale x-ray imaging of hot plasmas. Microscopy requires a distinct instrumental configuration that meets several constraints peculiar to that application, plus a complete rescaling of components. For example, grid arrangements must be reworked so as to provide a common field of view in a selected focal plane. Furthermore, alignment and control for microscope applications presents different requirements because the focal plane is a short distance from the instrument.

The NRL/LLNL collaboration covers design and fabrication of grid sets and supporting software for a prototype FTM to be used at LLNL. The grid system is designed to meet the requirements just mentioned. The software system currently simulates performance of the grid system and is also designed to support image reconstruction from data obtained with the grid system.

II. FTM THEORY

The principle of operation of the Fourier transform microscope can be understood by beginning with Fig. 1, which shows the overall instrument and depicts its major subassemblies. It shows that the system essentially consists of two grid assemblies $G1$ and $G2$, placed at distances D and L from the object to be imaged, plus a position-sensitive detector placed slightly behind $G2$. Both $G1$ and $G2$ consist of multiple small apertures containing grids with parallel ribs and spaces at various spacings and orientations. Each of these small apertures will be called a subgrid and the portion of the apparatus consisting of (i) one subgrid from $G1$, (ii) its corresponding subgrid from $G2$, and (iii) the portion of the detector that reads out photons from the source that have passed through these subgrids will be referred to as a "sub-grid system." The total instrument may be thought of as an ensemble of subgrid systems.

Each subgrid system measures the amplitude and phase of the Fourier transform of the source brightness distribution along a single direction α and for a single wave number k, where α is the angle the ribs make with the y axis of the instrument, and the wavelength $2\pi k^{-1}$ is the distance between rib centers as projected onto the source plane. The wave number vector (u,v) is related to k and α via $u=k\cos\alpha$, $v=k\sin\alpha$. Hence each subgrid system can be used to measure one Fourier component (amplitude and phase) from the two-dimensional Fourier transform of the image. From the set of Fourier amplitudes and phases the image is reconstructed.

The detector output can be thought of as a Fourier encoding of the image presented to the device, with each subgrid system providing the amplitude and phase at a particular point in the Fourier transform domain. The subgrid systems function as follows. Subgrid A in the $G1$ plane uses a number N of ribs to cover a specific solid angle as seen from the detector. This subgrid therefore projects one Fourier component out of the source, which is registered as a band of stripes on the corresponding subgrid B in the $G2$ plane. Subgrid B possesses $N+m$ ribs (where m is typically 1 or 2), and lies in that part of $G2$ where photons from the source that have passed through A have been projected. The flux of photons at the point (x',y') on the detector is obtained by integrating the *apparent* source intensity $I(x,y)W(x,y,x',y')$ over solid angles, where (x,y) is the position in the image plane and $W(x,y,x',y')$ is the transmission function for the subgrid system as viewed along the line of sight from (x',y') to (x,y). The combination of the two subgrids causes the throughput to be a Moiré pattern (with a number of maxima m), on which is superposed a modulation at a much higher spatial frequency (Fig. 2). The high-frequency modulation is not crucial and can be ignored.

The locations of maximum throughput relative to the boundaries of subgrid B specify the points where the transformed image projected by subgrid A is in phase with the fixed ribs of B. Subgrid B therefore functions rather like a vernier. The amplitude and phase of the Moiré pattern yield the Fourier components for the two-dimensional spatial frequency corresponding to the spacing and orientation of the subgrid system. The total ensemble of subgrid systems is chosen to provide sufficient coverage of the Fourier transform domain, so that the set of measurements provided by all of the subgrid systems will produce an image of suitable quality for the task. In general the more detailed the desired image the more subgrids that will be needed. The device provides magnification in the sense that measurement of the phase of the Moiré pattern (made on a

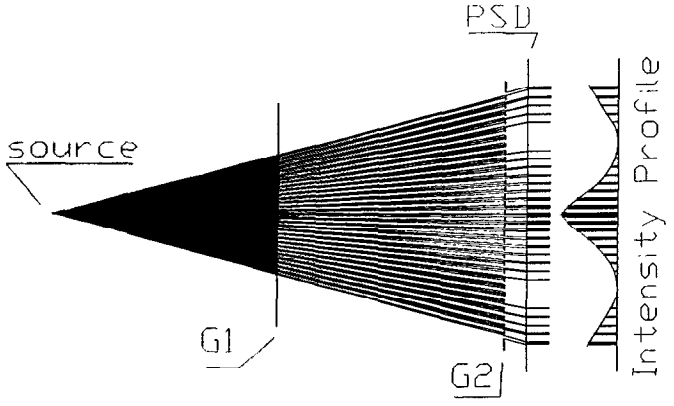

FIG. 2. Subgrid system.

scale of several hundred microns) yields information at the resolution scale of the microscope (a few microns). The position resolution required in the position-sensitive detector is on the order of 10% of the width of grid $G2$, although additional resolution beyond this can be exploited if it happens to be available.

III. IMPLEMENTATION: GRID LAYOUT

Mathematical specification of the desired grid system consists of enumerating which Fourier components are to have their amplitudes and phases measured. Many practical design issues remain beyond this point. One of these is the packing problem of finding an arrangement for the large number of subgrids on the two planes that lets each subgrid gather photons from the source without confusion from stray photons from other subgrid systems and with all subgrid systems viewing the same region in the focal plane. Figure 3 shows a representative grid layout satisfying these constraints. Note that all of the ribs are arranged radially to minimize vignetting. The central regions of $G1$ and $G2$ are reserved for Fresnel zone plates, used with a

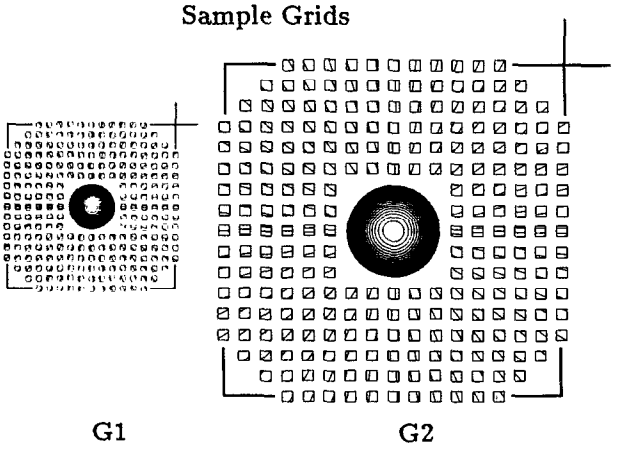

FIG. 3. Arrangement of subgrids on $G1$ and $G2$ satisfying the common field-of-view constraint for the case $L/D=2$ (see Fig. 1). Only rib orientations (and not spacings) are accurately portrayed. All of the ribs are arranged radially to minimize vignetting.

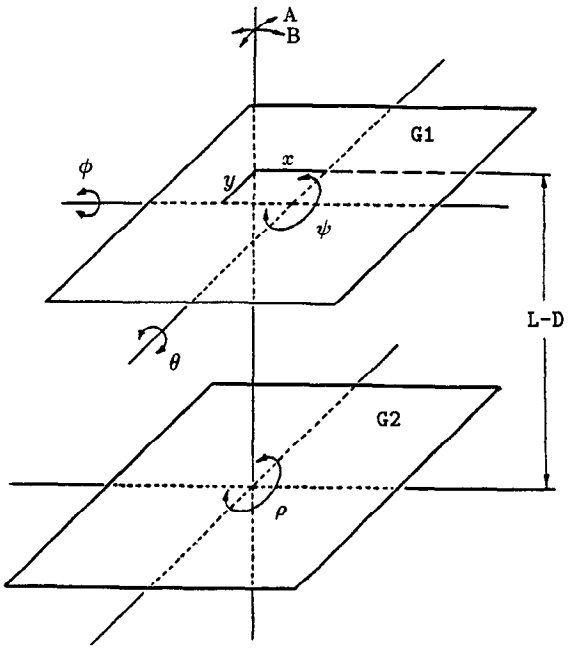

FIG. 4. Degrees of freedom of grid system.

visible light source for system alignment as explained below. This geometrical arrangement must then be realized with grids that have adequate opacity to photons at the intended operating energy. The grid system must not be affected by diffraction. This places a limit on how fine the grid spacing can be; the limit is $d^2 > \lambda L/2$, where L is the overall length of the system and λ is the longest wavelength at which it is to operate. In practice it is possible to build diffraction-limited systems at the lower energies but in gamma rays the limitation on spatial resolution is set by fabrication considerations combined with requirements for achieving adequate photon absorption in the grid ribs.

Design specification consequently includes the following information: (i) the size of the individual subgrids; (ii) the number of subgrids in each of the $G1$ and $G2$ grids; (iii) for each subgrid of $G1$ the dimensions of the ribs, their spacing, and their orientations relative to a chosen direction; (iv) the relative magnifications of the individual dimensions of a $G2$ subgrid relative to its counterpart in $G1$ (the orientation of the ribs will be identical in the two grids); (v) the coordinates of the centers of the individual $G1$ and $G2$ subgrids.

It is also necessary to include some scheme for alignment and calibration. In the NRL/LLNL prototype, system alignment is accomplished by placing Fresnel zone plates at the centers of $G1$ and $G2$. It will be noted that each of the grid planes has three rotational and three translational degrees of freedom. Figure 4 shows a convenient system for characterizing these degrees of freedom. The rear plane ($G2$) is taken to define the coordinate system used for the figure, hence its degrees of freedom are associated with the spatial placement and orientation of the entire apparatus. The angles θ and ϕ on the front ($G1$) plane and the translational degrees of freedom (x,y) of that same plane are controlled by mounting the grids in a rigid

optical bench. If this is not done aberrations can result, e.g., tilt of these planes distorts the apparent spatial wavelength. The separation between the planes, $L-D$, is also something that can be fixed rigidly, but if it is allowed to vary the system will behave like a zoom lens, allowing field of view and spatial resolution to scale. The instrument orientation is defined by the angles A and B. These angles are controlled by use of the alignment feature of the instrument, which employs the Fresnel zone plates for laser alignment.

The operational procedure for the FTM begins with an alignment and calibration. A laser is used to illuminate a small sphere placed at the source position and the Fresnel zone plate in $G1$ is then used to aim the apparatus precisely at the sphere. For x-ray calibration, a point source (e.g., a radioactive source placed behind a lead plate with a hole less than 1 resolution element in size) is placed at the target position. It is used to determine amplitudes and phases for all subgrids in the system. This set of measurements becomes the reference system for actual imaging. When calibration and alignment are complete the image-accumulation measurement (data run) may take place. In each subgrid the phase measured from the calibration run is subtracted off that from the data run. Calibration can be done at any time. It may be run off-line with the instrument at another site, provided all components are rigidly held in their relative positions between the calibration and data runs. Measured amplitudes and corrected phases from the data run are then passed to the mathematical inversion algorithm detailed below, which reconstructs the image.

IV. SIMULATIONS

Image reconstruction proceeds by feeding the measured amplitudes and phases to a software package that inverts and reconstructs the source map, or brightness distribution. Since the Fourier transform has been sampled, not fully measured, this reconstructed image involves deconvolution to remove the point source response of the subgrid system ensemble, typically in a maximum entropy image reconstruction approach.

At its core the image processing system is based upon Fourier transforms. The grid system records all or part of the Fourier transform of the source brightness distribution. The amplitude $\tilde{A}$ and phase Φ measured by a subgrid pair are equivalent to two components of the transform at a particular spatial frequency [i.e., $\tilde{A}\sin(kx+\Phi)$ can be thought of as being the same as $A_1\cos(kx)+A_2\sin(kx)$, where A_i are suitably defined]. A software system of this sort can be developed from a suitable Fourier transform package and then interfaced to the desired application. However, there exists a software package used for the deconvolution of interferometric data in radio astronomy called AIPS (for "Astronomical Image Processing System",[8]) which does essentially that task. It is transportable and comes with a user interface suitable for handling a variety of data inputs. We have used AIPS to perform the inverse transformation required to obtain the source brightness distribution. The inverse transformation algorithm was tested by simulating the projection of test images through the grid system and passing the amplitudes and phases to AIPS for inversion. The inverted image is then compared with the original test image.

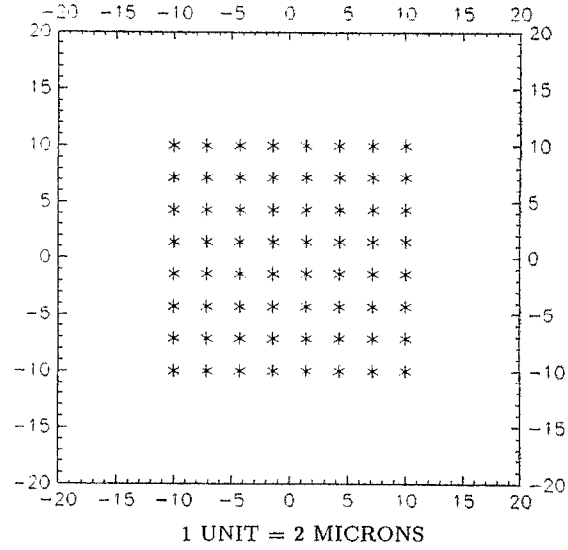

FIG. 5. Test image composed of 64 uniform points.

The instrument currently being fabricated comprises 240 subgrid systems, with a finest spacing of 2 μm. The predicted limit of resolution for this system is 4 μm for a 100-μm field of view. Sparse and dense point-source test patterns were used to simulate the instrument response. Figure 5 depicts a test image composed of 64-point sources arrayed in a uniform square pattern with 40-μm sides. Figure 6 depicts the AIPS-inverted image as a perspective plot. The individual peaks corresponding to the points in the test image can be clearly seen. The limit of resolution is not approached in the 64-point test (Figs. 5 and 6) since the spacing between points is roughly 6 μm. In Fig. 7 we document the simulated resolution for two point sources spaced 4 μm apart, by taking slices through the inverted image. The intensity distribution satisfies the predicted Rayleigh criterion. A limitation of the current instrument

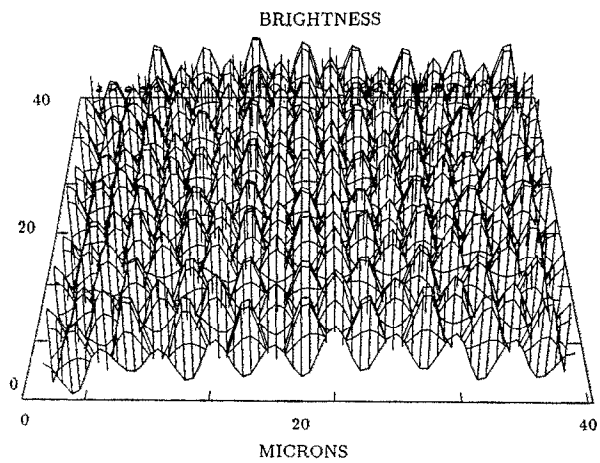

FIG. 6. Inverted image of 64 uniform points.

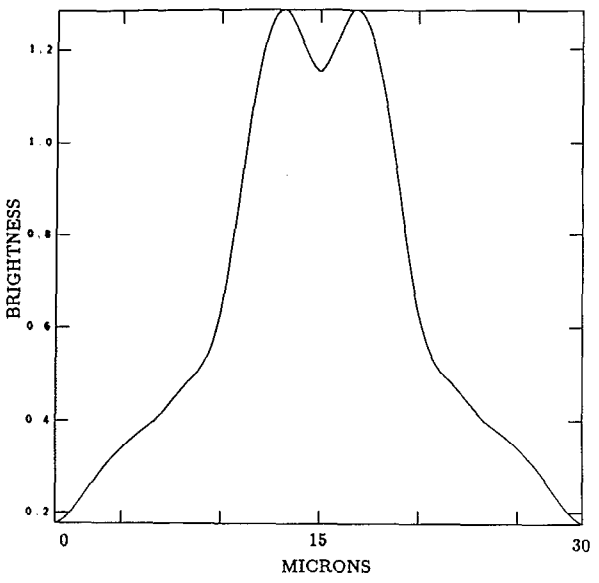

FIG. 7. Slice through inverted image of two points with 4-μm spacing.

simulation system is that the input is restricted to distributions of point sources.

V. CONCLUSION

The FTM concept is workable either in hard x rays (>3 keV) or gamma rays. Below about 3 keV other techniques are adequate. The choice of operating energy dictates materials, fabrication methods, and limiting spatial resolution. Diffraction-limited imaging is possible for energies up to about 10 keV, beyond which the requirement for absorbing photons in grid ribs sets the scale for the rib thickness and consequently determines inter-rib spacing as well, from a practical fabrication standpoint.

The main advantage of this family of microscopes consists of ability to provide high-spatial-resolution imaging in hard x rays and gamma rays. The finest spatial scale that can be mapped depends on the energy of the photons used, but is approximately 1 μm for 3-keV x rays and approximately 50-μm for gamma rays above 100 keV. Such a capability has not existed previously. The magnification inherent in the two-grid approach places minimal positional resolution requirements on the detector.

[1] L. Mertz, *Transformations in Optics* (Wiley, New York, 1965).
[2] R. H. Dicke, Ap. J. (Lett.), **153**, L101 (1968).
[3] W. N. Christiansen and J. A. Hogbom, *Radiotelescopes* (Cambridge, New York, 1969).
[4] J. D. Kraus, *Radio Astronomy* (McGraw-Hill, New York, 1966).
[5] M. Oda, Appl. Opt. **4**, 143 (1965).
[6] H. Bradt *et al.* Space Sci. Rev. **8**, 471 (1968).
[7] T. Kosugi, *et al.* in *The Yohkoh (Solar-A) Mission* (Kluwer Academic, London, 1991).
[8] A. Bridle, *AIPS Cookbook* (NRAO, Charlottesville, VA, 1985).